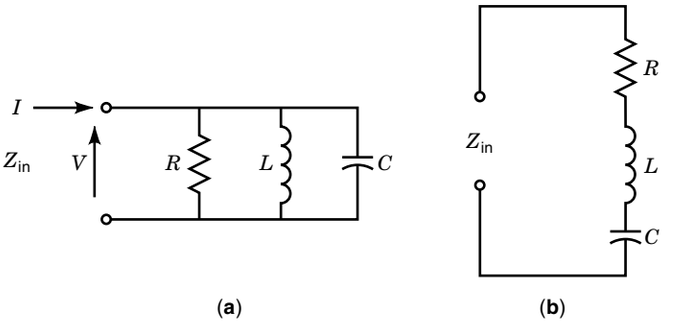

Figure 1. Lumped element (a) parallel and (b) series resonant circuits.

CAVITY RESONATORS

RESONANT STRUCTURES

Resonant structures are network elements that are used extensively in the development of various microwave components (1). At low frequencies, resonant structures are invariably composed of lumped elements. As frequencies increase, lumped-element resonant circuits are attained by using transmission lines. Microwave resonant structures are almost invariably understood as cavity resonators. Conventional resonators consist of a bounded electromagnetic field in a volume enclosed by metallic walls. The electric and magnetic energies are stored in the electric and magnetic fields, respectively, of the electromagnetic fields inside the cavity and the equivalent lumped inductance and capacitance of the structure can be determined from the respective stored energy. It is important to note that cavity resonators, in contrast to lumped resonators, have an infinite number of resonant frequencies (or modes). In the vacinity of each resonant frequency, the cavity can be approximated by an associated lumped equivalent circuit.

Some energy is dissipated as finite conductivity of the metallic walls and the equivalent resistance can therefore be determined from the currents flowing on the walls of the cavity resonator (2,3). In this chapter, a brief description of the cavity resonators most commonly employed in various microwave components is presented. As far as possible, simple expressions have been provided for design applications. Basic parameters of microwave resonators are first presented because they describe a cavity. Then, various coaxial and waveguide resonators are described. Fabrication, coupling, measurements, and applications of cavity resonators are also included.

RESONATOR PARAMETERS

Resonant Frequency

The parameters of a resonator at microwave frequencies are essentially similar to those of a lumped-element resonator circuit at low frequencies. They can easily be described using an *RLC* series or parallel network. Consider, for instance, an *RLC* parallel network as shown in Fig. 1(a). The input impedance of such a network as a function of frequency has both real and imaginary parts. At resonance, the input impedance is real and is equal to the resistance of the circuit. The electric and magnetic stored energies are also equal, leading to the expression for the resonant frequency as

$$\omega_0 = \frac{1}{\sqrt{LC}} \tag{1}$$

Quality Factor

The performance of a resonant circuit is described in terms of the quality factor Q, and such features as frequency selectivity, bandwidth, and damping factors can be deduced from this. The quality factor is defined as

$$Q = \omega \frac{\text{time-averaged stored energy}}{\text{energy lost per second}} \tag{2}$$

for the lumped resonant circuits,

$$Q = \omega RC = \frac{R}{\omega L} \tag{3}$$

for the parallel network Fig. 1(a), and

$$Q = \frac{1}{\omega CR} = \frac{\omega L}{R} \tag{4}$$

for the series network Fig. 1(b).

Fractional Bandwidth

The input impedance of the parallel resonant circuit of Fig. 1 is given by

$$Z_{\text{in}} = \left[\frac{1}{R} + \frac{1}{j\omega L} + j\omega C\right]^{-1} \tag{5}$$

At a frequency $\omega_0 \pm \Delta\omega$ in the vicinity of the resonant frequency, Eq. (5) reduces to

$$Z_{\text{in}} = \frac{R}{1 \pm j2Q(\Delta\omega/\omega_0)} \tag{6}$$

From Eq. (6), it is clear that at $\omega = \omega_0$ the input impedance is only resistive. However, when

$$\Delta\omega = \frac{\omega_0}{2Q} \tag{7}$$

the magnitude of the input impedance decreases to $R\sqrt{2}$ of its maximum value R, and the phase angle is $\pi/4$ for $\omega < \omega_0$ and $-\pi/4$ for $\omega > \omega_0$. From Eq. (7), the fractional bandwidth BW is defined as

$$\mathrm{BW} = \frac{2\Delta\omega}{\omega_0} = \frac{1}{Q} \tag{8}$$

Loaded Quality Factor

In practical situations, the resonant circuit is coupled to an external load R_L that also dissipates power, and the loaded quality factor Q_L is given by

$$\frac{1}{Q_\mathrm{L}} = \frac{1}{Q} + \frac{1}{Q_\mathrm{e}} \tag{9}$$

where Q_e is the external quality factor for a lossless resonator in the presence of the load.

Damping Factor

Another important parameter associated with a resonant circuit is the damping factor δ_d. It is a measure of the rate of decay of the oscillations in the absence of an exciting source. For high Q resonant circuits, the rate at which the stored energy decays is proportional to the average energy stored. Consequently, the stored energy as a function of time is given by

$$W = W_0 e^{-2\delta_\mathrm{d} t} = W_0 e^{-\omega_0 t/Q} \tag{10}$$

which implies that

$$\delta_\mathrm{d} = \frac{\omega_0}{2Q} \tag{11}$$

Thus, we see that the damping factor is inversely proportional to the Q of the resonant circuit. In the presence of an external load, the Q should be replaced by Q_L.

Alternately, the input impedance in the vicinity of resonance Z_in given by Eq. (6) can be rewritten to take into account the effect of losses in terms of the complex resonant frequency

$$\omega_\mathrm{c} = \omega_0 + j\delta_\mathrm{d} = \omega_0\left(1 + j\frac{1}{2Q}\right) \tag{12}$$

so that

$$Z_\mathrm{in} = \frac{\omega_0 R/(2Q)}{j(\omega - \omega_\mathrm{c})} \tag{13}$$

In Eq. (13) the parameter R/Q is called the figure of merit and describes the effect of the cavity on the gain bandwidth product. In terms of the lumped elements of the resonant circuit,

$$\frac{R}{Q} = \sqrt{\frac{L}{C}} \tag{14}$$

COAXIAL CAVITY RESONATORS

At microwave frequencies, the dimensions of lumped resonator circuits become comparable to the wavelength, and this may cause energy loss by radiation. Therefore, resonant circuits at these frequencies are shielded to prevent radiation. Perfectly conducting enclosures, or cavities, provide a means of confining energy. Usually, cavities with the largest possible surface area for the current path are preferred for low-loss operation, and the energy is coupled to them by the various means described later in this chapter.

Coaxial Resonators

A coaxial cavity resonator (Fig. 2) supporting TEM (Transverse Electromagnetic) waves can easily be formed by a shorted section of coaxial line. Resonances appear whenever the length d of the cavity is an integral number of half-wavelengths. The resonance modes occur at

$$f = \frac{nc}{2d}, \quad n = 1, 2, \ldots \tag{15}$$

where c is the speed of light. The lowest resonant frequency corresponds to $n = 1$, and the Q of the cavity for this mode is given by (4)

$$Q\frac{\delta}{\lambda_0} = \frac{1}{4 + 2(d/b)(1 + b/a)/\ln(b/a)} \tag{16}$$

where δ is the skin depth and a and b are inner and outer radii, respectively. It is also possible to have higher-order resonance modes, depending on the structural parameters of the coaxial line. The first higher-order mode appears when the average circumference is equal to the wavelength in the dielectric medium of the line. The cutoff frequency of this mode is

$$f_\mathrm{c} = \frac{c}{\pi\sqrt{\epsilon_\mathrm{r}}(a + b)} \tag{17}$$

where ϵ_r is the dielectric constant of the medium. Other higher-order modes correspond to TE (Transverse Electric) and TM (Transverse Magnetic) waves that exist in a circular

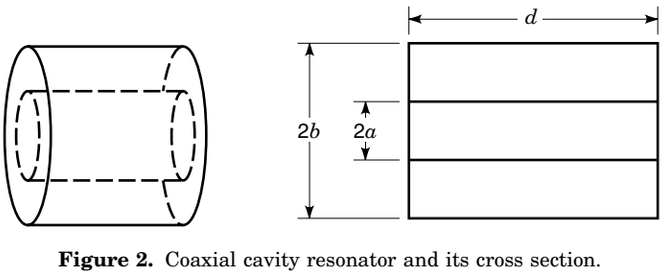

Figure 2. Coaxial cavity resonator and its cross section.

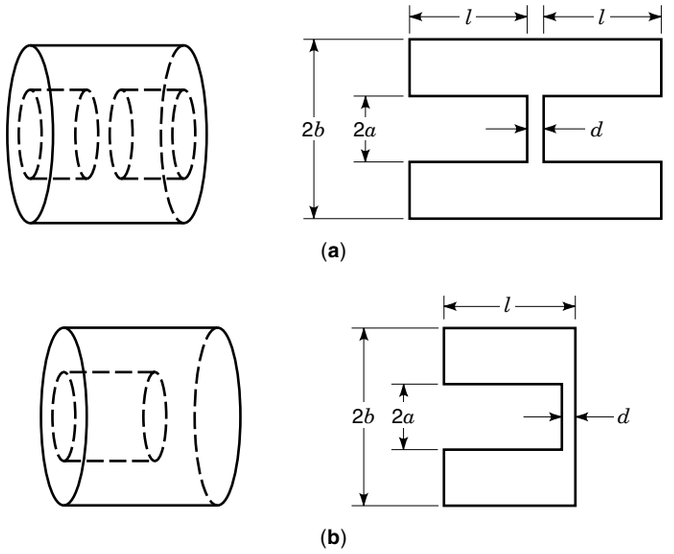

Figure 3. Re-entrant coaxial cavity resonators. (a) Capacitively loaded coaxial cavity resonator. (b) Radial-cavity resonators.

waveguide with the radius of the center conductor approaching zero. The resonance condition is

$$k_{nml} = \left[p_{nm}^2 + \left(\frac{l\pi}{2d} \right)^2 \right]^{1/2} \tag{18}$$

where $k_{nml} = 2\pi f_{nml}/c$ and p_{nm} is the cutoff wavenumber that is obtained as the mth root of the transcendental equations,

$$J_n'(ka)N_n'(kb) - J_n'(kb)N_n'(ka) = 0 \tag{19}$$

for TE modes, and

$$J_n(ka)N_n(kb) - J_n(kb)N_n(ka) = 0 \tag{20}$$

for TM modes. Here J_n and N_n are the nth-order Bessel functions of the first and second kind, respectively, and the prime denotes their derivatives with respect to their arguments.

Reentrant Coaxial Resonators

Another coaxial cavity configuration consists of a short section of coaxial line with a gap in the center conductor. Figure 3(a) shows a capacitively loaded coaxial cavity. Radial cavity as shown in Fig. 3(b) is another possible variation. They are also referred to as reentrant coaxial cavities because the metallic boundaries extend into the interior of the cavity. They are widely used in microwave tubes. The resonant frequency of such a structure can be evaluated from the solution of the transcendental equation (21),

$$\tan \beta l = \frac{dc}{\omega a^2 \ln(b/a)} \tag{21}$$

where d is the gap in center conductor, and $2l + d$ is the length of the cavity. From Eq. (21), it is obvious that the capacitively loaded coaxial cavity can have an infinite number of modes. For the radial reentrant cavity of Fig. 3(b), the resonant frequency can be evaluated by calculating the inductance and capacitance of the structure. The expression for the resonant frequency is

$$f = \frac{c}{2\pi\sqrt{\epsilon_r}} \left[al \left(\frac{a}{2d} - \frac{2}{l} \ln \frac{0.765}{\sqrt{l^2 + (b-a)^2}} \right) \ln \frac{b}{a} \right]^{-1/2} \tag{22}$$

An approximate expression for the Q of the cavity is

$$Q \frac{\delta}{\lambda_0} = \frac{2l}{\lambda} \frac{\ln(b/a)}{2\ln(b/a) + l[(1/a) + (1/b)]} \tag{23}$$

for a tunable reentrant cavity, d is large, and $(l - d)$ is also large compared with b. The resonances occur whenever the length of the center conductor is approximately a quarter wavelength.

Annular Coaxial Resonator

An annular coaxial resonator is formed by a figure of revolution of a coaxial radial-cavity resonator (refer to Fig. 3) about an axis that is offset from and parallel to the center conductor (5). As shown in Fig. 4, the electric field in the plane containing the axis is similar to that of the radial-cavity resonator. The electric field in the plane normal to the axis is radial and is same along the circumference. In effect, the annular resonator is equivalent to a half wavelength coaxial resonator with a small shunt capacitance in the middle. One of the important application of this type of resonator is that it can be coupled simultaneously with several sources. The electric field at the gap is quite high and results in good coupling to external sources.

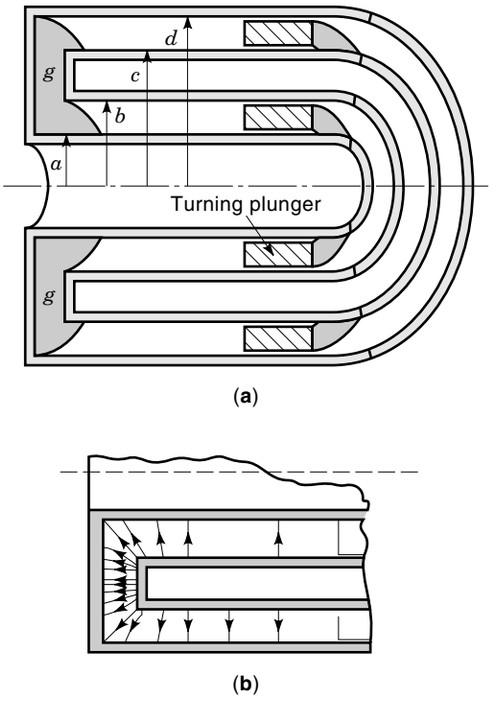

Figure 4. Two views of annular coaxial resonator structure.

WAVEGUIDE CAVITIES

Rectangular Waveguide Resonators

Rectangular resonant cavities are formed by a section of rectangular waveguide of length d. This cavity can also support an infinite number of modes. The field configuration of the standing wave pattern for the incident and reflected wave is not unique, that is, it depends on the assumed direction of propagation of the wave. In order to be consistent, we shall assume that wave propagation is in the positive z direction. The standing wave pattern is then formed by the incident and reflected waves traveling in $+z$ and $-z$ directions, respectively. The cutoff wavenumber k_{cmn} is given by

$$k_{cmn}^2 = \left(\frac{m\pi}{a}\right)^2 + \left(\frac{n\pi}{b}\right)^2, \quad m = 0, 1, 2, \ldots, \quad n = 0, 1, 2, \ldots \tag{24}$$

where a and b are waveguide dimensions. The resonant wavenumber is then expressed as

$$k_{mnp} = \left[\left(\frac{m\pi}{a}\right)^2 + \left(\frac{n\pi}{b}\right)^2 + \left(\frac{p\pi}{d}\right)^2\right]^{1/2}, \quad p = 1, 2, \ldots \tag{25}$$

and the resonant frequency is defined as

$$f_{mnp} = \frac{k_{mnp}c}{2\pi} \tag{26}$$

From the preceding discussion, we see that the resonant frequency is the same for TE and TM modes. Therefore, they are referred to as degenerate modes. The field configuration of the dominant TE_{101} mode is shown in Fig. 5(b). The quality factor Q of the dominant TE_{101} mode in the rectangular resonant cavity having surface resistance R_s can be evaluated using the expression

$$Q = \frac{120\pi^2}{4R_s}\left[\frac{2b(a^2+d^2)^{3/2}}{ad(a^2+d^2)+2b(a^3+b^3)}\right] \tag{27}$$

In rectangular cavities, the resonant frequency increases for higher-order modes, as does the Q at a given frequency. Higher-order mode cavity or "echo boxes" are useful in applications where a slow rate of decay of the energy stored in the cavity after it has been excited is required.

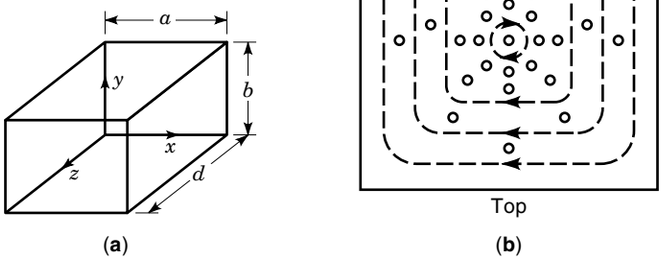

Figure 5. (a) Rectangular waveguide cavity resonator. (b) Field configuration of the dominant TE_{101} mode.

Circular Waveguide Resonators

Circular waveguide cavities are most useful in various microwave applications. Most commonly, they are used in wavemeters to measure frequency, have a high Q factor, and provide greater resolution. These consist of a section of circular waveguides of radius a and length d as shown in Fig. 6.

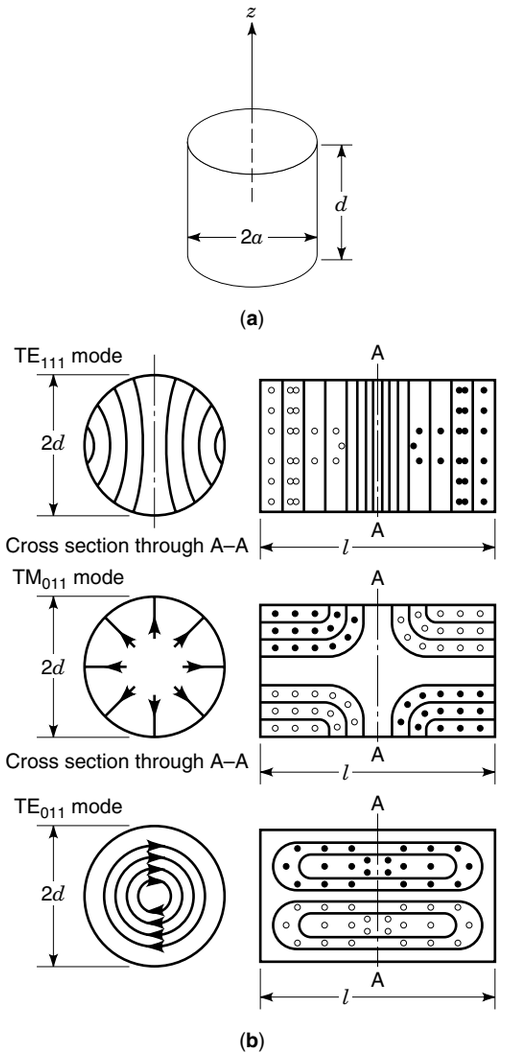

Figure 6. (a) Circular cylindrical waveguide cavity resonator. (b) Field configurations for TE_{111}, TM_{011}, and TE_{011} modes in cylindrical cavities.

Table 1. Roots of the Transcendental Equation $J_n'(ka) = 0$

Modes		
n	m	p'_{nm}
0	1	0.0
1	1	1.841
2	1	3.054
0	2	3.832
3	1	4.201
4	1	5.318

The resonance wavenumber of the circular waveguide cavity is given by

$$k_{nml} = \left[\left(\frac{x_{nm}}{a} \right)^2 + \left(\frac{l\pi}{d} \right)^2 \right]^{1/2}, \quad l = 0, 1, 2, \ldots \tag{28}$$

where

$$x_{nm} = \begin{cases} p'_{nm} & \text{for TE modes} \\ p_{nm} & \text{for TM modes} \end{cases} \tag{29}$$

Values for p'_{nm} for various modes are given in Table 1. Field lines for TE_{111}, TM_{011}, TE_{011} modes are shown in Fig. 6. Simplifying Eq. (28) yields

$$(2af_{nml})^2 = \left(\frac{cx_{nm}}{\pi} \right)^2 + \left(\frac{cl}{2} \right)^2 \left(\frac{2a}{d} \right)^2 \tag{30}$$

The Q of the circular cavity for TE_{nml} modes can be evaluated from

$$Q \frac{\delta}{\lambda_0} = \frac{[1 - (n/p'_{nm})^2][(p'_{nm})^2 + (l\pi a/d)^2]^{3/2}}{2\pi[(p'^2_{nm} + 2a/d(l\pi a/d)^2 + (1 - 2a/d)(nl\pi a/p'_{nm}d)^2]} \tag{31}$$

and for the dominant TE_{111} mode, Q can be obtained by substituting $n = m = l = 1$ in the preceding equation. Using Eq. (30), plots of $(2af)^2$ versus $(2a/d)^2$ can be used to construct mode charts, as shown in Fig. 7. From this it can be seen that, for the TE_{011} mode operation, the safe value of $(2a/d)^2$ is between 2 and 3. For TM model operation, the Q is given by

$$Q \frac{\delta}{\lambda_0} = \begin{cases} \dfrac{[p_{nm}^2 + (l\pi a/d)^2]^{1/2}}{2\pi(1 + 2a/d)} & \text{for } l > 0 \\ \dfrac{p_{nm}}{2\pi(1 + a/d)} & \text{for } l = 0 \end{cases} \tag{32}$$

As with rectangular cavity resonators, the Q is higher for higher-order modes.

Elliptic Waveguide Resonators

Elliptic resonant cavities that are formed using a section of an elliptic waveguide offer several advantages. There is no mode splitting caused by slight deformations in the cavity surface, and the electric field configuration in the transverse plane is fixed with respect to its axes. Also, the longitudinal electric field of the TM_{111} mode in an elliptic cavity with semimajor axis a is always greater than the circular cavity with radius a. This feature may be useful in the dielectric material characterization that uses perturbation techniques (6).

The elliptic waveguide supports four different types of modes, namely, even TE and TM modes and odd TE and TM modes. The TE modes have $E_z = 0$ and the TM modes have $H_z = 0$. From the solution of wave equation, there exist four different modes. The modes having cosine type variation are called even modes and the modes having sine type variation are called odd modes. The subscript c and s are added to the mode designation to describe this variation.

The elliptic waveguide in Fig. 8(a) is shown along with the orthogonal elliptic coordinate system. As can be seen, the confocal elliptic cylinders are formed with constant ξ, and confocal hyperbolic cylinders are formed with constant η. The distance between the two foci, F and F' is $2h$. The outer wall of the elliptic waveguide is formed with $\xi = \xi_0$. The semimajor axis is then

$$2a = 2h \cosh \xi_0 \tag{33}$$

and, the semiminor axis is

$$2b = 2h \sinh \xi_0 \tag{34}$$

Alternatively, the eccentricity e is

$$e = 1/\cosh \xi_0 = \sqrt{1 - (b/a)^2} \tag{35}$$

The resonance wavenumber for elliptic cavity is given by

$$k_{rmnl} = \left[\left(\frac{2\sqrt{x_{rmn}}}{ae} \right)^2 + \left(\frac{l\pi}{d} \right)^2 \right]^{1/2}, \quad l = 0, 1, 2, \ldots \tag{36}$$

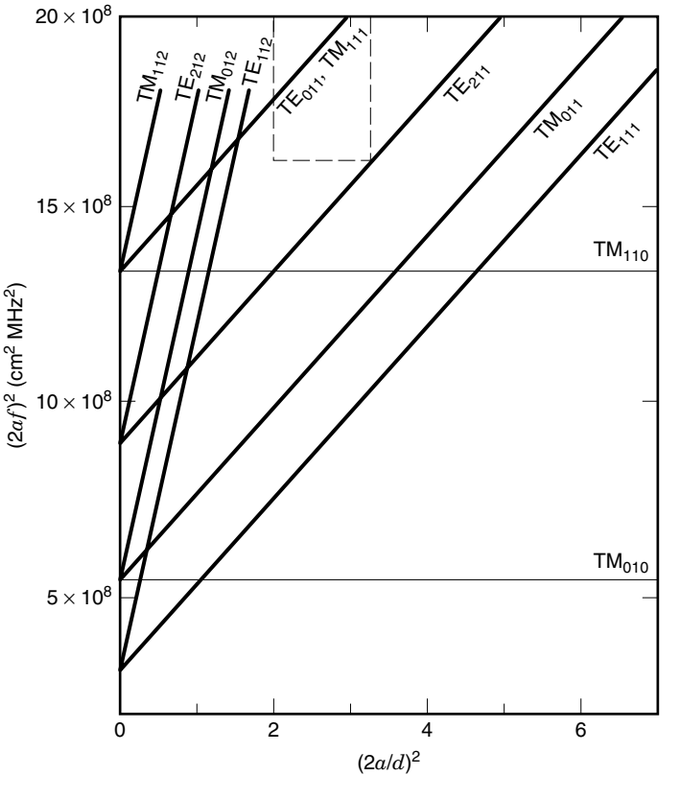

Figure 7. Mode chart of a circular cylindrical cavity resonator.

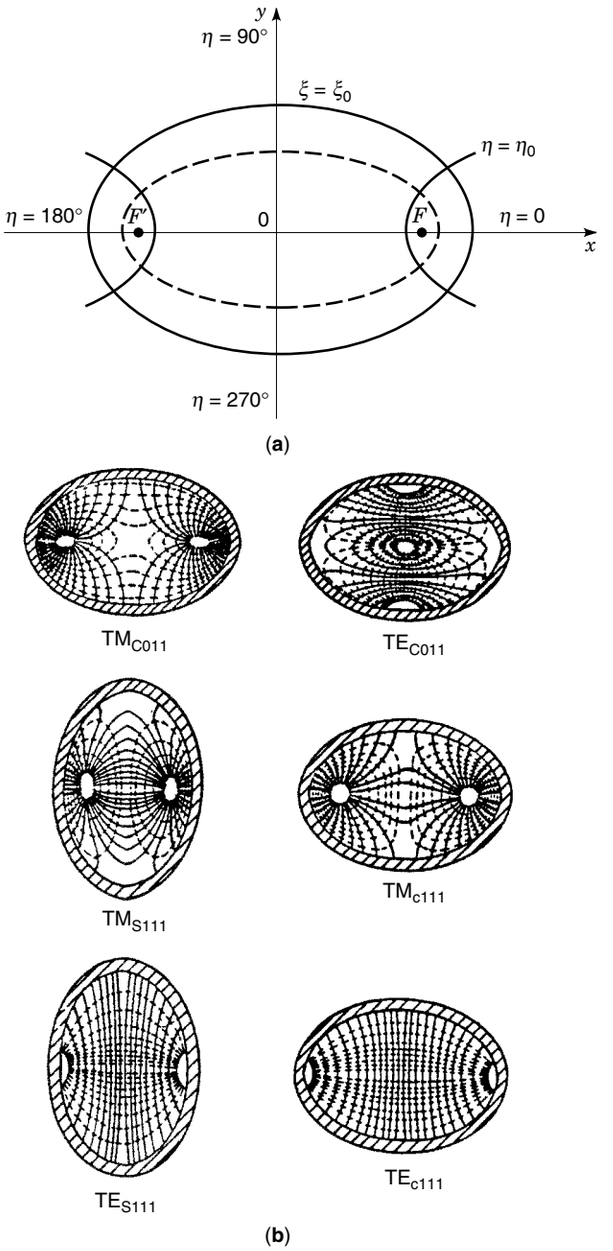

Figure 8. (a) Elliptic waveguide cavity resonator. (b) Field configuration for some modes in elliptical cavities.

where

$$x_{rmn} = \begin{cases} q'_{rmn} & \text{for TE}_{rmn}\text{ modes} \\ q_{rmn} & \text{for TM}_{rmn}\text{ modes} \end{cases} \tag{37}$$

In Eq. (37), r can be substituted with c and s to obtain even and odd modes, respectively. The parameter $q_{cmn}(q_{smn})$ is the nth parametic zero of the even (odd) modified Mathieu function of order m with argument ξ_0 and is used to calculate $\text{TM}_{cmn}(\text{TM}_{smn})$ modes. Similarly, for a $\text{TE}_{cmn}(\text{TE}_{smn})$ mode, the parameter $q'_{cmn}(q'_{smn})$ is the nth parametic zero of the first derivative of the even (odd) modified Mathieu function of order m with argument ξ_0 and is used to calculate $\text{TE}_{cmn}(\text{TE}_{smn})$ modes. The equations used to find the parametric zeros are given next (7).

$$\begin{aligned} \text{TM modes:}\quad & Ce_m(\xi_0, q) = 0 \text{ even} \\ & Se_m(\xi_0, q) = 0 \text{ odd} \\ \text{TE modes:}\quad & Ce'_m(\xi_0, q) = 0 \text{ even} \\ & Se'_m(\xi_0, q) = 0 \text{ odd} \end{aligned} \tag{38}$$

Field lines for some modes are shown in Fig. 8(b).

Annular Elliptic Resonator

The annular elliptic waveguide in Fig. 9(a) is shown along with the orthogonal elliptic coordinate system. The outer ellipse with eccentricity e_0 and the inner ellipse with eccentricity e_1 form a confocal annular elliptic waveguide. The distance between the two foci F and F' is $2h$ and is related to the other structural parameters via the relation

$$2h = 2a_0e_0 = 2a_1e_1 \tag{39}$$

where a_0 and a_1 are the semimajor axes of the outer and inner ellipse, respectively. Alternatively, the eccentricities e_0 and e_1 are also expressed as

$$e_0 = 1/\cosh\xi_0 = \sqrt{1 - (b_0/a_0)^2} \tag{40}$$

and

$$e_1 = 1/\cosh\xi_1 = \sqrt{1 - (b_1/a_1)^2} \tag{41}$$

where b_0 and b_1 are the semiminor axes of the outer and inner ellipses, respectively. The axial coordinates of the outer and inner ellipses are ξ_0 and ξ_1.

In a manner similar to the elliptic waveguide, the eigenvalue equation for annular elliptic waveguide was solved by Bräckelmann (8). The relevant equations for TM and TE modes follow.

Even modes, TE_{cmn}:

$$Ce'_m(\xi_0, q_{cmn})Fey'_m(\xi_1, q_{cmn}) - Ce'_m(\xi_1, q_{cmn})Fey'_m(\xi_0, q_{cmn}) = 0 \tag{42}$$

Odd modes, TE_{smn}:

$$Se'_m(\xi_0, q_{smn})Gey'_m(\xi_1, q_{smn}) - Se'_m(\xi_1, q_{smn})Fey'_m(\xi_0, q_{smn}) = 0 \tag{43}$$

Even modes, TM_{cmn}:

$$Ce_m(\xi_0, q_{cmn})Fey_m(\xi_1, q_{cmn}) - Ce_m(\xi_1, q_{cmn})Fey_m(\xi_0, q_{cmn}) = 0 \tag{44}$$

Odd modes, TM_{smn}:

$$Se_m(\xi_0, q_{smn})Gey_m(\xi_1, q_{smn}) - Se_m(\xi_1, q_{smn})Fey_m(\xi_0, q_{smn}) = 0 \tag{45}$$

In Eqs. (42)–(45), $Ce_m(\xi, q)$ and $Se_m(\xi, q)$ are the even and odd modified Mathieu functions of the first kind and order m. $Fey_m(\xi, q)$ and $Gey_m(\xi, q)$ are the even and odd modified Mathieu functions of the second kind and order m (9). The

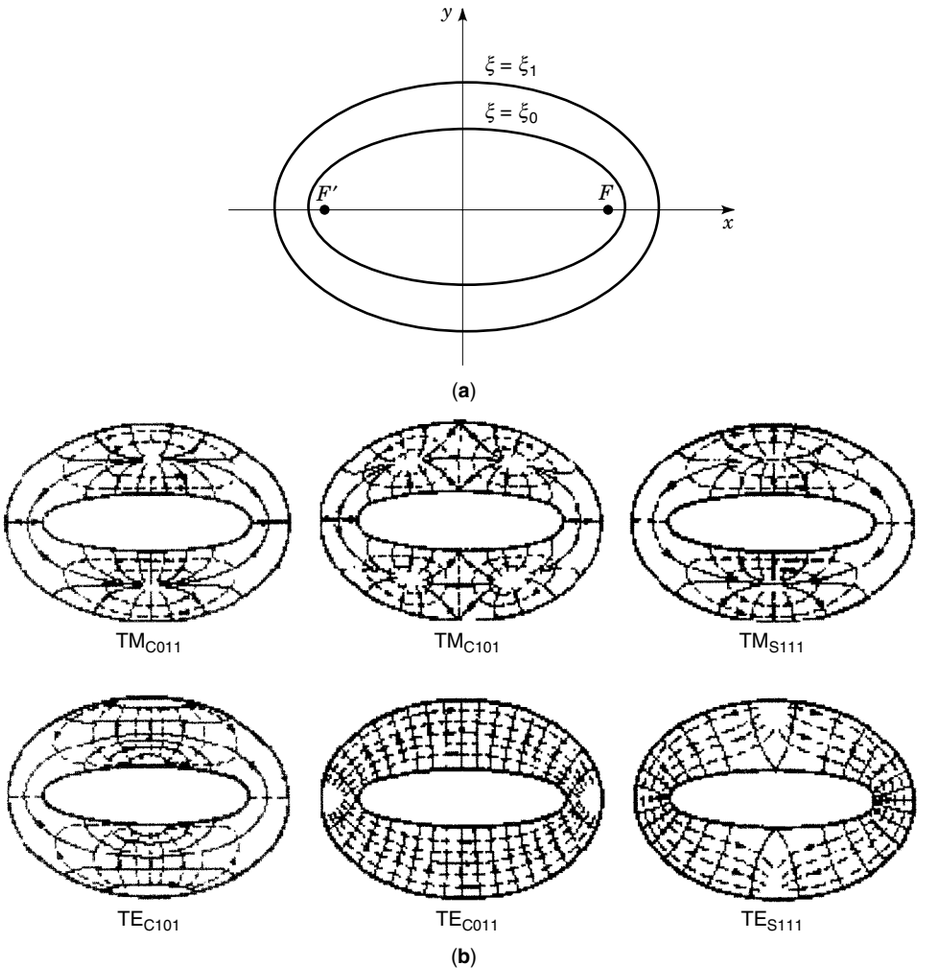

Figure 9. (a) Annular elliptic cavity resonator. (b) Field configuration for some modes in annular elliptic cavities.

primes in Eqs. (42)–(45) denote the derivative with respect to the argument ξ. The parameter q'_{cmn} is the nth parametic zero of Eq. (42), and q_{cmn} is the nth parametric zero of Eq. (44). Similar explanation applies for (Eqs. 43) and (45) for the odd TE and TM modes.

The resonance wavenumber for annular elliptic cavity is given by

$$k_{rmnl} = \left[\left(\frac{2\sqrt{x_{rmn}}}{ae} \right)^2 + \left(\frac{l\pi}{d} \right)^2 \right]^{1/2}, \quad l = 0, 1, 2, \ldots \tag{46}$$

where

$$x_{rmn} = \begin{cases} q'_{rmn} & \text{for TE}_{rmn} \text{ modes} \\ q_{rmn} & \text{for TM}_{rmn} \text{ modes} \end{cases} \tag{47}$$

The annular elliptic resonators also supports four different types of modes, namely, even TE and TM modes and odd TE and TM modes. Field lines for some modes are shown in Fig. 9(b).

Spherical Resonators

Another cavity resonator shape is the spherical resonator. Based on the solution of Maxwell's equations in the spherical coordinate system, the axial symmetry results in TM modes containing E_r, E_θ, H_ϕ, and TE modes containing H_r, H_θ, E_ϕ. Because the origin is included inside the hollow spherical cavity, the resonance condition is easily obtained by setting $E_\theta = 0$ at $r = a$, where a is the radius of the sphere.

Solution of transcedental equation

$$\tan ka = \frac{ka}{1 - (ka)^2} \tag{48}$$

results in dominant TM_{101} resonance at

$$\lambda_0 = 2.29a \tag{49}$$

and the second TM_{102} resonance at a wavelength of

$$\lambda_0 = 1.4a \tag{50}$$

The modes in a spherical cavity are shown graphically in Fig. 10.

The Q of a spherical cavity operating in the dominant mode is

$$Q \frac{\delta}{\lambda_0} = 0.318 \tag{51}$$

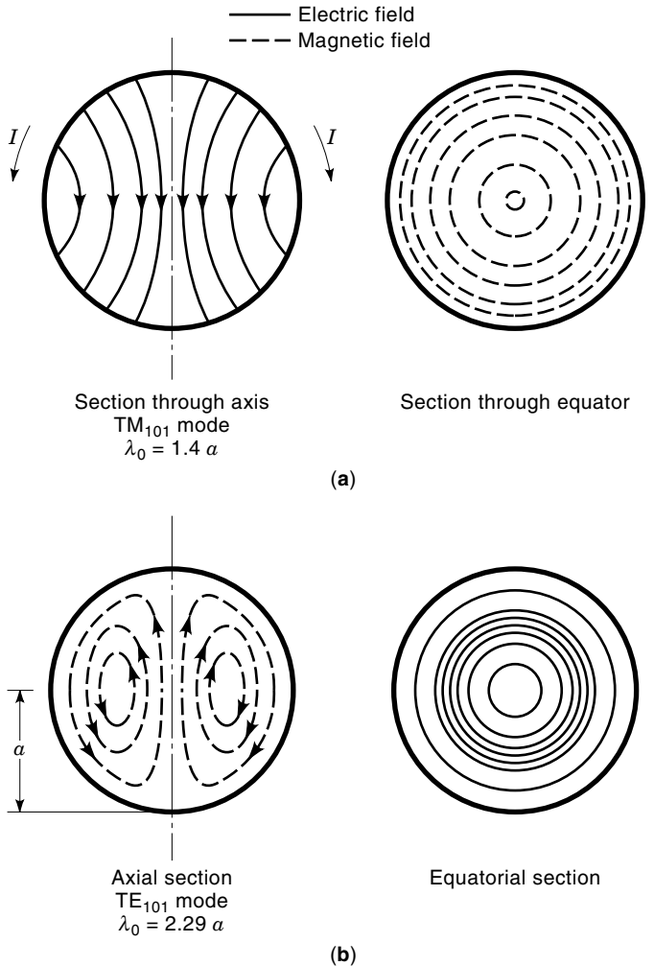

Figure 10. Fields in a spherical cavity resonator at the first and second resonant frequency.

and the equivalent shunt resistance is simply

$$R\frac{\delta}{\lambda_0} = 104.4 \tag{52}$$

Spherical Resonators with Reentrant Cones

Spherical resonators with reentrant cones were found to be suitable for realizing oscillators for klystrons (10).

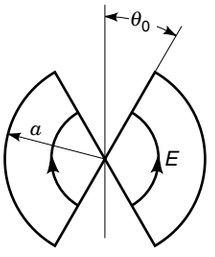

Figure 11. Spherical resonator with re-entrant cones and fields in the fundamental modes.

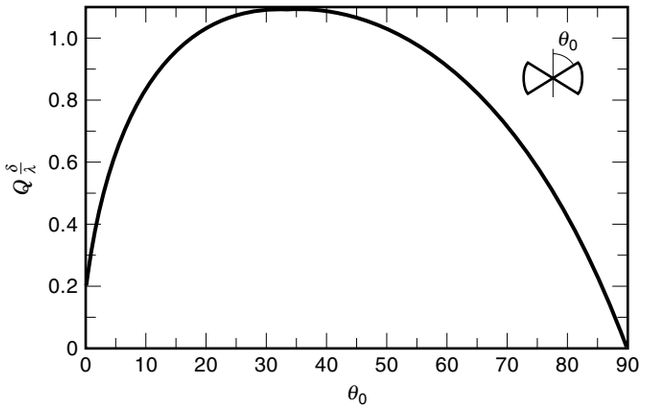

Figure 12. $Q(\delta/\lambda_0)$ for a spherical resonator with re-entrant cones.

It consists of a hollow conducting sphere of radius a and two cones whose apex is at the center of the sphere and subtends an angle of $2\theta_0$. Its structure and fundamental mode fields are shown in Fig. 11.

The resonant wavelength is not a function of θ, as is the case in spherical resonators. The resonant wavelength is

$$\lambda_0 = 4a \tag{53}$$

However Q and R of the resonator are functions of the angle θ. The plots of $Q(\delta/\lambda_0)$ and $R(\delta/\lambda_0)$ are given in Ref. 4 and are given in Figs. 12 and 13, respectively.

As can be seen, the maximum Q is obtained at $\theta = 34°$ and is given by

$$Q\frac{\delta}{\lambda_0} = 0.1095 \tag{54}$$

and the maximum R occurs at $\theta = 9°$ and is given by

$$R\frac{\delta}{\lambda_0} = 32.04 \tag{55}$$

Ellipsoid-Hyperbolic Waveguide Resonators

Another cavity resonator suitable for klystrons is of ellipsoid–hyperboloid shape. This shape is a figure of revolution about the axis passing through its foci, as shown in Fig. 14. The

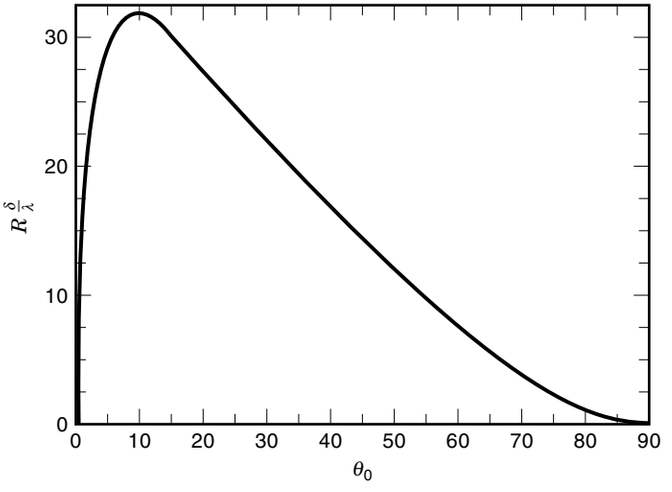

Figure 13. $R(\delta/\lambda_0)$ of a spherical resonator with re-entrant cones.

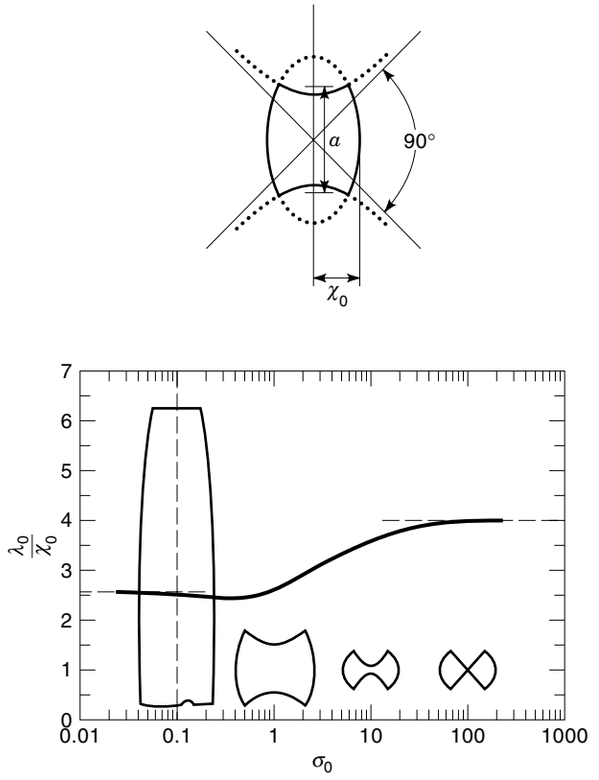

Figure 14. Ellipsoid–hyperboloid resonator and normalized resonant wavelength λ_0/b as a function of shape factor $\sigma_0 = 2b/a$.

distance between foci a as well as the hyperboloid that determines part of the resonator is held constant. The normalized resonant wavelength λ_0/b, where b is the equitorial radius, is plotted as a function of the shape factor $\sigma_0 = 2b/a$. Interestingly, the shape of the resonators vary widely as the shape factor is increased. Both the Q as well as R are function of the shape factor. The $Q(\delta/\lambda_0)$ and $R(\delta/\lambda_0)$ (given in Ref. 4) are plotted as a function of shape factor in Figs. 15 and 16, respectively.

Arbitrary Shaped Resonators

The early work in microwaves focused on analytical and numerical solutions of hollow waveguide problems. Most of the

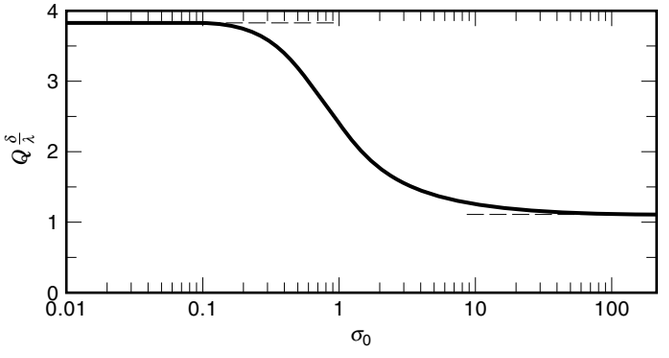

Figure 15. $Q(\delta/\lambda_0)$ of an ellipsoid-hyperboloid resonator as a function of shape factor $\sigma_0 = 2b/a$.

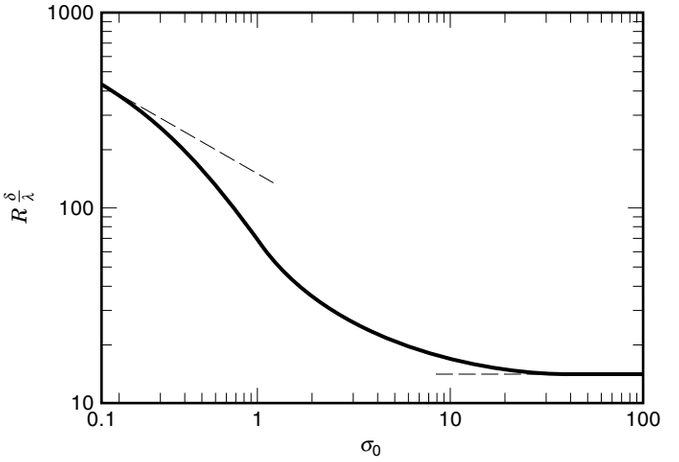

Figure 16. $R(\delta/\lambda_0)$ of an ellipsoid–hyperboloid resonator as a function of shape factor $\sigma_0 = 2b/a$.

attempts were to solve them for TE and TM modes, either exactly or approximately. Ng (11) compiled the methods used to calculate the cutoff wavenumbers of hollow waveguides. As pointed out there, three basic cross-sectional shapes can be distinguished:

1. Convex shape
2. Nonconvex with smooth reentrant portion
3. Nonconvex with sharp reentrant portion

A resonant structure can be formed using any one of them by closing the hollow waveguide with end walls. The cutoff wavenumbers can be found using references given in Table II of Ref. 11. The resonant frequency can be easily calculated. The basic equation to use is

$$k = \frac{2\pi f_0}{c} = \left[(k_c)^2 + \left(\frac{l\pi}{d}\right)^2\right]^{1/2}, \quad l = 0, 1, 2, \ldots \tag{56}$$

FABRICATION

Materials

Microwave and millimeter-wave cavities are usually made from the same material used for the waveguide such as copper, brass, or aluminum. In order to provide low-loss characteristics, the interior (and exterior) is plated with low-loss materials such as silver and gold.

There exists a wide range of waveguide sizes to cover frequencies from as low as 400 MHz to 200 GHz. The operating bandwidth of the waveguide increases as the frequency increases. Therefore, the method of fabrication is very important in realizing low loss or high Q cavities.

Cavities are formed using short sections of waveguides. There are various approaches used in their fabrication. The waveguide tubing formed using extrusion process generally provides various dimensional tolerances varying from 0.008 in. (0.2 mm) to 0.001 in. (0.025 mm). In order to realize accurate waveguide dimensions, particularly at millimeter wave-

lengths, the process of electroforming is generally used. A conducting or nonconducting mandrel is used as a starting material in the electroforming process. The mandrel is later removed to leave the electroformed waveguide. Special grade stainless steel mandrels with high surface finish can be used to electroform the waveguide. They are removed by heating and applying uniform force. Nonconducting mandrels formed using plastics or highly compressed wax can be used to form complicated cross sections. Such mandrels can be chemically dissolved to retain the final form of the electroformed waveguide.

In most applications, the waveguide must interact with cavities to realize the prescribed description of the component. Fabrication from a solid metal block using a milling process is preferred because it provides an integrated component for some complicated waveguide assemblies. This approach reduces reflections and spurious transmission by minimizing interfaces or flanges.

Cavity Perturbation

At resonance the cavity contains equal amounts of average electric and magnetic energy. Any perturbation in the structural dimensions or imperfections in the cavity wall will require readjustment in resonant frequency such that the electric and magnetic energies are equal. It is possible to measure accurately the frequency shift $\Delta\omega/\omega$, which can be used to determine other parameters of the cavity (2).

Effect of Temperature and Humidity

The resonant frequencies of a cavity resonator depends on the dimensional variations of the material used in the construction as well as on the variations in the dielectric constant.

As temperature changes, the dimensions of the cavity change in accordance with the thermal expansion coefficient of the material used in its construction. The change in the resonant frequency can be easily determined using the equation for the resonant frequency for a given cavity structure. This change can be minimized by bimetals with a lower coefficient of thermal expansion.

Furthermore, the dielectric constant of the air within an unsealed cavity also varies depending on the temperature, atmospheric pressure, and humidity level.

Tunable Cavities

Various microwave and millimeter-wave applications require resonators that can be tuned frequently and at high speeds. Both contacting as well as noncontacting plungers are used to tune cavity resonators.

Contacting Plunger. A movable short circuit is provided by the direct contact between the plunger and the cavity walls. The plunger is typically a quarter wavelength long at the center frequency. In order to provide good electrical contact, the contacting plungers, as shown in Fig. 17, have axial serrations. These serrated fingers maintain sufficient pressure to scratch off any insulating film formed inside the cavity walls. Because the contact is made at or near a current node, the losses are minimized. In some cases, particularly for millimeter-wave applications, a metal shoulder is also added to move the short circuit reference plane forward. In this case, the actual contact is not at or near a current node.

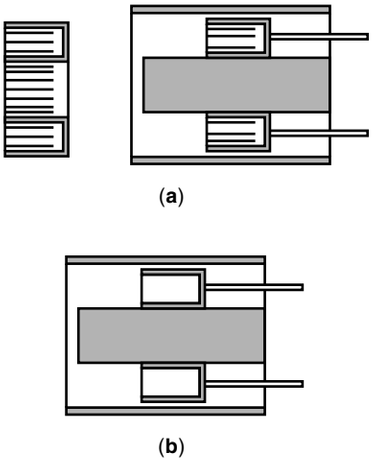

Figure 17. Contacting plunger.

Contacting resonators have several disadvantages, such as

- They provide erratic contact due to small metal particles and nonsmooth cavity interior walls.
- They are not repeatable because of the backlash in the mechanical driving mechanism as well as the friction between the contacting surfaces.
- The contact causes wear and produces an insulating film, which results in increased contact resistance. The increases losses will result in lower Q of the cavity.

Noncontacting Plunger. The disadvantages of the contacting plungers can be eliminated by using noncontacting plungers. These plungers provide a near short circuit over a wider frequency range. The impedance at the face of the plunger is a complex impedance with a low value of resistance. The capacitive, choke, or bucket-type plungers, as shown in Fig. 18, provide reasonable performance (5). Multisection plungers are formed by quarter-wavelength low–high–low impedance sections. The leakage through these sections may cause parasitic resonance; therefore, the back of the plunger section must be terminated in the characteristic impedance of the transmission line used to realize the cavity.

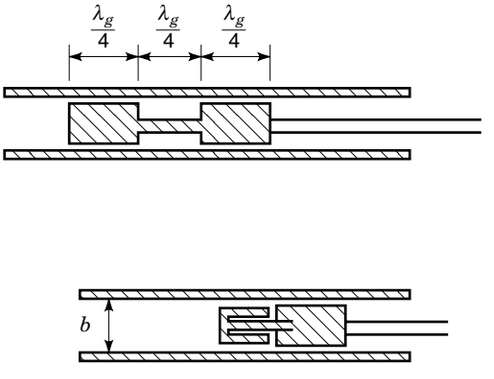

Figure 18. Noncontacting plunger.

COUPLING INTO AND OUT OF CAVITIES

As we have seen, the cavities are essentially enclosed structures. In order to use them, we must couple them to transmission lines. We can use the coaxial line or any form of waveguide to couple power into and out of the cavities. In this sense, the input and output coupling structures act as a load on the cavity. The cavity parameters, such as resonant frequency and Q, are invariably affected by the presence of these structures. The resonant behavior of the cavities is exploited extensively in the realization of filters with prescribed functional forms.

Coupling

Coupling structures provide a means of coupling energy into and/or out of the cavity. The excitation of the cavity can be accomplished by electric or magnetic coupling. In case of electric coupling, the electric field of the coupling structure is parallel to the electric field of the cavity. The magnetic coupling is provided when the magnetic field of the coupling structure is parallel to the magnetic field of the cavity.

The coaxial line can be used to provide either electric or magnetic coupling.

1. *Electric Probes.* The center conductor of the coaxial line acts as a probe. Its direction is parallel to the direction of the electric field in the cavity.
2. *Current Loops.* The center conductor of the coaxial line is terminated in a short-circuit to form a loop. The loop produces a magnetic field perpendicular to the plane of the probe and in the same direction as the magnetic field in the cavity.

Cavities are also excited by waveguides though apertures formed by holes and slits (Fig. 19). The coupling mechanism can be of electric or magnetic type.

1. *Magnetic Coupling Apertures.* The aperture is located between the cavity and input waveguide such that the magnetic field in the waveguide is parallel to the magnetic field in the cavity. Round holes in the wall separating the waveguide and cavity provide magnetic coupling.
2. *Electric Coupling Apertures.* The aperture is located between the cavity and input waveguide such that the electric field in the waveguide is normal to the electric field in the cavity. A narrow slot in the wall separating the waveguide and cavity can provide electric coupling.

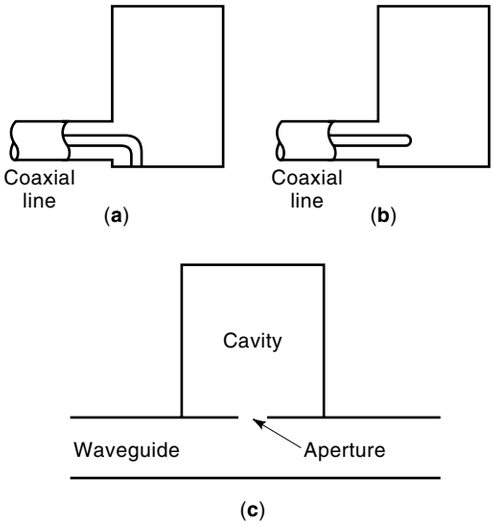

Figure 19. Cavity excitation using (a) loop coupling, (b) electric probe coupling, and (c) aperture coupling.

Coupling Through Probes

One popular approach used to transfer energy from a coaxial line to a waveguide is by electric probes. In a typical configuration, the axis of the coaxial line is perpendicular to the broadside of the rectangular waveguide. The center conductor of the coaxial line protrudes through the waveguide wall and extends into the waveguide. The outer conductor of the coaxial line is terminated at the waveguide wall. The electric fields from the end of the center conductor terminate on the other broadside wall parallel to the dominant E field of the waveguide. They are, therefore, called electric probes. If the probe is shaped to form a circular loop and the end of the probe is terminated on the broad wall of the waveguide, the current flow through this loop will induce a magnetic field parallel to the dominant H field of the waveguide. In this case, the probe is a magnetic current loop.

In an electric probe, the center conductor of the coaxial line forms a radiating antenna. Depending on the length or depth of this section, the input impedance at the interface can be inductive or capacitive. For optimum performance, the antenna should present a matched load at the interface. The probe excites waveguide modes that propagate in both directions; therefore, the energy is divided equally in both directions. In order to redirect the energy in the preferred direction, the other side is terminated in a short circuit. In the case of rectangular waveguide cavities, the placement of the probe is determined from one of the shorted ends. Invariably, a tunable short will be required for optimum transfer of power. The probe can be constructed with various lengths and diameters. The distance between the probe and the short circuit is determined experimentally.

The bandwidth of the probe can be improved by providing a broadband match at the interface. This can be achieved by changing the length and diameter of the probe. Other approaches include making the end round, attaching a metal sphere at the end, or flaring the center conductor. If direct current (dc) return is desired, the probe can be terminated on the other broadwall, or it can rest on a cross-bar across the waveguide broad dimension. Sometimes the probe is extended through the opposite side of the waveguide to form another section of shorted coaxial line. The position of the short in this case provides an additional variable.

The input impedance of a short diameter coaxial antenna is given by

$$Z_{\text{in}} \cong l^2 \cos^2 \frac{\pi x_0}{a} \sin^2 \frac{2\pi x_1}{\lambda_g} - jX \tag{57}$$

where l is length of the probe, x_0 is the distance from the center of the waveguide, and x_1 is the distance from the probe

to the short. The value of the reactance is large implying that the input impedance has a large capacitive component.

Coupling Holes in Waveguides

The coupling from a waveguide to a cavity can be provided by apertures consisting of holes and slits. The aperture can be infinitesimally thin or with finite thickness. The insertion loss caused by a hole of finite thickness t is given by

$$\alpha_T = \alpha_b + \alpha_t \tag{58}$$

where α_b is the attenuation resulting from the susceptance of the hole, and α_t is the attenuation in the below cutoff waveguide hole.

Holes in a Rectangular Waveguide. For a hole of diameter d in a rectangular waveguide normal to the direction of propagation, the normalized susceptance B is given by

$$\frac{B}{Y_0} \cong \frac{3}{2\pi}\frac{ab\lambda_g}{d^3} \tag{59}$$

where Y_0 is the characteristic admittance of the dominant waveguide mode, and λ_g is the guide wavelength of a waveguide having broadside dimension a and smaller dimension b.

The attenuation α_b resulting from the hole is

$$\alpha_b = 20\log\frac{B}{2Y_0} \tag{60}$$

and the attenuation resulting from the finite thickness α_t is

$$\alpha_t = 32\sqrt{1-\left(1.706\frac{d}{\lambda}\right)^2}\frac{t}{d} \cong 32\frac{t}{d}\,\text{dB} \tag{61}$$

where λ is the operating wavelength.

Holes in a Circular Waveguide. For a hole of diameter d normal to the direction of propagation in a circular waveguide of diameter $2a$, the normalized susceptance B is given by

$$\frac{B}{Y_0} = \frac{\lambda_g}{4a}\left(5.71\frac{a^3}{d^3} - 2.344\right) \tag{62}$$

where Y_0 is the characteristic admittance of the dominant waveguide mode, and λ_g is the guide wavelength of the dominant mode.

The attenuation α_b resulting from the hole is

$$\alpha_b = 10\log\left[\frac{(B/Y_0)^2}{4} - 1\right]\text{dB} \tag{63}$$

and the attenuation α_t resulting from the finite thickness is given by Eq. (61), and the total attenuation is calculated using Eq. (58).

RESONATOR MEASUREMENTS

As described earlier, the resonator is described fully in terms of the resonant frequency f_0, the coupling coefficient, and the quality factors. The unloaded quality factor Q_u, loaded quality factor Q_L, and external quality factor Q_e are useful in various circuit analyses containing microwave cavities.

Experimental determination of the parameters is straightforward using modern microwave network analyzers. In Fig. 20, a single-port and two-port cavity measurement set-ups are shown. The magnitude and phase of the reflection and transmission coefficients are measured to determine the resonator parameters.

Single-Port Resonator

The equivalent circuit of a single-port cavity resonator is shown in Fig. 1, where R, L, and C are the equivalent lumped resistance, inductance, and capacitance. The equivalent parallel and series circuits of Fig. 1(a) and (b) are also known as the detuned short and open configurations, respectively. The equivalence between series and shunt parameters of these resonant circuits is as shown in the following table.

Parameter	Series Tuned	Parallel Tuned
f_0	$\frac{1}{\sqrt{LC}}$	$\frac{1}{\sqrt{LC}}$
Q_u	$\frac{\omega L}{R}$	$\frac{R}{\omega L}$
β	$\frac{Z_0}{R}$	$\frac{R}{Z_0}$
Q_L	$\frac{Q_u}{1+\beta}$	$\frac{Q_u}{1+\beta}$

The input impedance of the circuit in Fig. 1(a) can be rewritten as

$$Z_{in} = \frac{R}{1 + j2Q_u\delta} \tag{64}$$

where $\delta = (\omega - \omega_0)/\omega_0$ represents the frequency detuning parameter (12). By varying δ, the locus of the impedance given by Eq. (64) is determined. On a Smith chart, a circular locus,

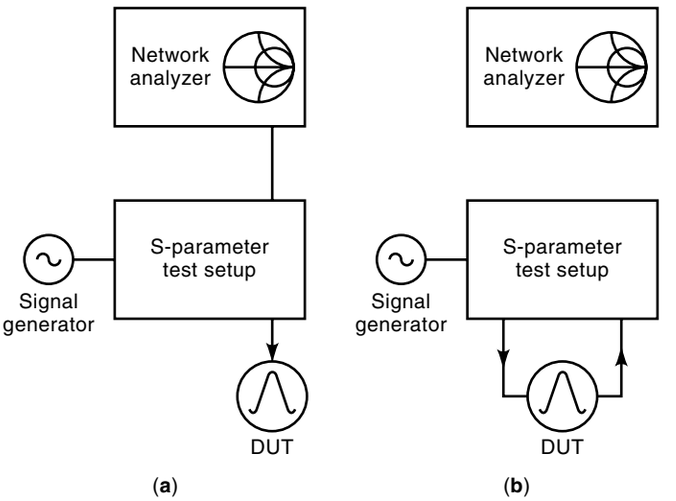

Figure 20. Measurement setup for (a) reflection and (b) transmission resonator.

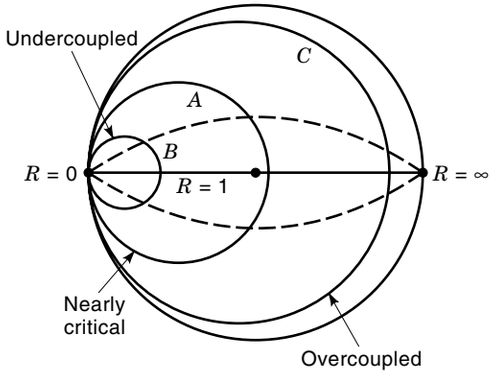

Figure 21. Input impedance of a single-port resonant cavity on the Smith chart for three degrees of coupling.

as shown in Fig. 21 is obtained depending on the coupling coefficient. For circle A, $R = Z_0$ and the locus passes through the origin. This condition is called critical coupling and corresponds to $\beta = 1$, implying that it provides a perfect match to the transmission line at resonance. The circle B with $R < Z_0$ is called undercoupled condition and $\beta < 1$. Finally, the circle C with $R > Z_0$ is an overcoupled condition with $\beta > 1$ (13).

The coupling coefficient for any cavity is calculated using the measurement of reflection coefficient S_{11,ω_0} at resonance. For the undercoupled case,

$$\beta = \frac{1 - S_{11,\omega_0}}{1 + S_{11,\omega_0}} \tag{65}$$

and for the overcoupled case,

$$\beta = \frac{1 + S_{11,\omega_0}}{1 - S_{11,\omega_0}} \tag{66}$$

The intersection of the impedance locus with the real axis provides the value of β as shown in Fig. 22.

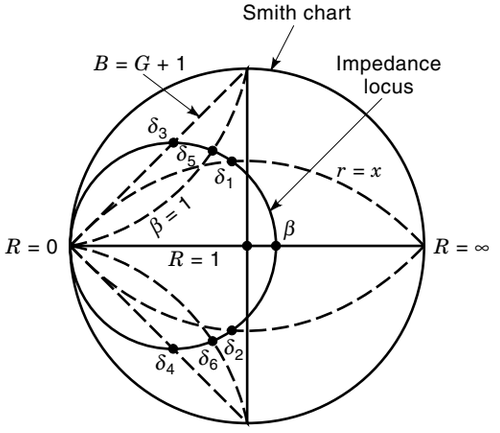

Figure 22. Determination of β and the half power points from the Smith chart. Q_0 locus is given by $X = R(B = G)$; Q_L by $X = R + 1$; Q'_{ext} by $X = 1$.

Other quality factors can be determined from Eq. (64), which can be rewritten as

$$\overline{Z}_{in} = \frac{Z_{in}}{Z_0} = \frac{\beta}{1 + j2Q_u\delta} = \frac{\beta}{1 + j2Q_L(1+\beta)} = \frac{\beta}{1 + j2Q_e\beta} \tag{67}$$

The Q_u, Q_L, and Q_e are related as

$$Q_u = Q_L(1 + \beta) = Q_e\beta \tag{68}$$

The normalized frequency deviations for unloaded, loaded, and external quality factors are given by

$$\delta_u = \pm\frac{1}{2Q_u}, \delta_L = \pm\frac{1}{2Q_L}, \text{and } \delta_e = \pm\frac{1}{2Q_e} \tag{69}$$

From Eqs. (69) and (67), the impedance locus of Q_u is determined and is given by

$$(Z_{in})_u = \frac{\beta}{1 \pm j} \tag{70}$$

Equation (70) represents the points on the impedance locus where the real and imaginary parts of the impedance are the same. Figure 22 represents the locus of these points (corresponding to $R = X$) for all possible values of β. This locus is an arc whose center is at $Z = 0 \pm j$, and the radius is the distance to the point $0 \pm j$. The intersection of this arc with the impedance locus determines the Q_u measurement points:

$$Q_u = \frac{f_0}{f_1 - f_2} \tag{71}$$

The frequencies f_1 and f_2 are called half-power points because these points correspond to $R = X$ on the impedance locus. The loaded and external Q values can be determined in a similar way. Equations (67) and (69), the impedances corresponding to Q_e and Q_L, are given by

$$(Z_{in})_e = \frac{\beta}{1 \pm j\beta} \tag{72}$$

and

$$(Z_{in})_L = \frac{\beta}{1 \pm j(1+\beta)} \tag{73}$$

By using Eqs. (72) and (73), the Q_e and Q_L loci are easily determined. These loci are shown in Fig. 22.

Two-Port Resonator

The equivalent circuit of a two-port cavity resonator is shown in Fig. 23. In this case, the input and output coupling are represented as β_1 and β_2. They are determined from

$$\beta_1 = \frac{Y_{01}}{n_1^2 G} \quad \text{and} \quad \beta_2 = \frac{Y_{02}}{n_2^2 G} \tag{74}$$

where Y_{01} and Y_{02} are the admittances seen at the input and output ports. The coupling coefficients are directly determined by measuring the VSWR at the input and output ports with the other port open circuited.

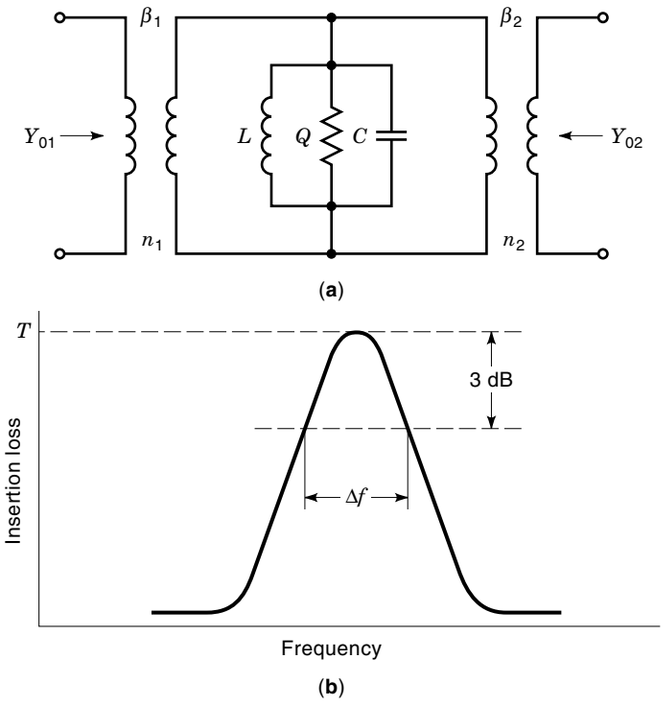

Figure 23. Equivalent circuit of a two-port resonator with input and output transformers. (b) Transmission response of a two-port resonator.

The transmission response of such a resonant circuit measured using the setup of Fig. 20, is shown in Fig. 23. The coupling coefficients and the quality factors for two-port resonators determined from the measurement of the insertion loss T at resonant frequency and the 3-dB bandwidth Δf using the following well-known relations (14)

$$T = \frac{2\sqrt{\beta_1 \beta_2}}{1 + \beta_1 + \beta_2} \tag{75}$$

$$Q_{\mathrm{L}} = \frac{f_0}{\Delta f} \tag{76}$$

$$Q_{\mathrm{u}} = Q_{\mathrm{L}}(1 + \beta_1 + \beta_2) \tag{77}$$

APPLICATIONS

A development of the cavity resonators was an important milestone in microwave technology. Early work on cavity resonators focused on cavities of regular shapes. But the development of microwave oscillators and amplifiers required complex shapes to achieve the performance required in the development of klystrons, magnetrons, and traveling wave tubes. Some of those shapes were covered in this chapter to illustrate the fact that different cavity structures are required to achieve the desired results.

Cavity resonators are also used extensively to measure frequency or wavelength. Tunable cavities are made to resonate at different frequencies by varying size and then calibrating size against frequency.

Cavity resonators are now most widely used to develop filters. Depending on the characteristics of the cavity, it can be used for narrowband as well as wideband filters. The applications of cavity resonators are concomitant with those of filters. In that sense, cavity resonators have applications in low-pass, band-pass, band-stop, and high-pass filters. They are also used in diplexers, multiplexers, and directional filters.

In the following sections, the preceding applications will be reviewed and their key aspects will be highlighted. Additional information can be found in other relevant sections of this encyclopedia.

Applications in Microwave Tubes

There were many problems in the early development of microwave valves that were caused by circuit elements and their interconnections. The development of resonant cavities led to the invention of klystron. The cavity resonators were able to reduce the transit time. The capacitance between the cathode and grid was used to resonate with the low inductance provided by the cavity.

In klystron amplifiers, multiple cavities are used to allow bunching of electrons. Because the electromagnetic fields in a cavity are changing as a function of time, the alternating electric fields at the grid cause bunching of electrons. By using another cavity at an optimum distance, the electrons are further bunched to build up oscillations. The first "buncher" resonator is excited into resonance through external means, and the second "catcher" resonator takes out the power. In klystron amplifiers, internal feedback is also provided via openings in the cavities.

In the reflex klystron, the electron beam is bunched by passing through a single resonator. The reflector returns the electron beam to this cavity at an optimum bunched condition. At this time, the energy is extracted from the cavity.

Magnetrons use various shapes of cavities to build oscillations and power. The power is extracted from one of the resonators through a coupling loop or an iris.

In traveling wave tubes, cavities are used as part of the slow wave structure. For additional information, refer to the appropriate section in this encyclopedia.

Filters

In order to use cavity resonators in filter applications, a reactance or susceptance slope parameter is generally required. The reactance slope parameter for a series resonant structure is defined as

$$\chi = \frac{\omega_0}{2} \frac{dX}{d\omega}\bigg|_{\omega=\omega_0} \text{ ohms} \tag{78}$$

Similarly, the susceptance slope parameter for the parallel resonant structure is defined as

$$B = \frac{\omega_0}{2} \frac{dG}{d\omega}\bigg|_{\omega=\omega_0} \text{ siemens} \tag{79}$$

From Eqs. (78) and (79), it is straightforward to see that for a series resonant circuit at resonance

$$\chi = \omega_0 L = \frac{1}{\omega_0 C} \tag{80}$$

and

$$Q = \frac{\chi}{R} \tag{81}$$

Similarly, for a parallel resonant circuit at resonance

$$B = \omega_0 C = \frac{1}{\omega_0 L} \tag{82}$$

and

$$Q = \frac{B}{G} \tag{83}$$

In a bandpass filter design, impedance or admittance inverters can be used with series or shunt-type resonant structures. The reactance or admittance slope parameter is related to filter prototype element values. The external Q and coupling coefficients are also expressed in terms of the reactance or admittance slope parameter. Inductive posts or irises with impedance inverters can be used to make a bandpass filter. For details on waveguide filters, refer to the appropriate section in this encyclopedia.

Measurement of Frequency

Both coaxial and waveguide resonators have been used in commercially available wavemeters. The main requirement in selecting cavity dimensions is to ensure that the cavity resonates in the fundamental mode, that there are no degenerate modes, and that they are easy to manufacture and calibrate.

These wavemeters are basically tunable cavities, and when the length is $\lambda_g/2$, the cavity resonates by taking in some energy from the transmission line, coaxial or waveguide. This action will produce a dip in the transmitted power. When the length of the cavity is calibrated, the frequency or wavelength can be read off directly from the dial. The extent of the dip depends on the amount of coupling. The Q of wavemeter cavities is quite high, on the order of 5000 to 10,000 depending on the desired accuracy.

In a coaxial line wavemeter, as shown in Fig. 24, the center conductor is used as a probe to couple energy to the resonator. Noncontacting plungers with chokes are used to provide a variable short position. The coaxial resonator will resonate

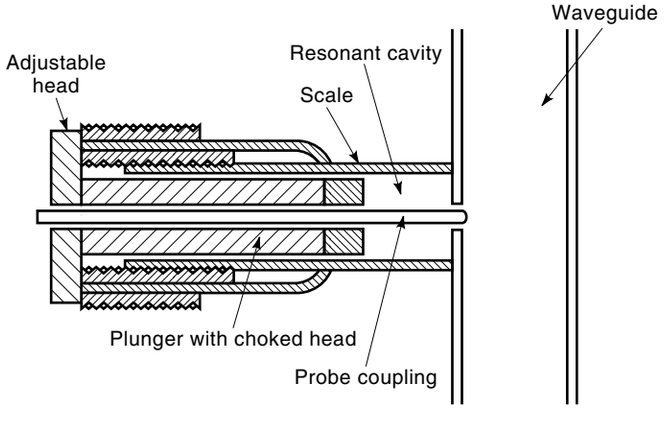

Figure 24. Coaxial cavity wavemeter.

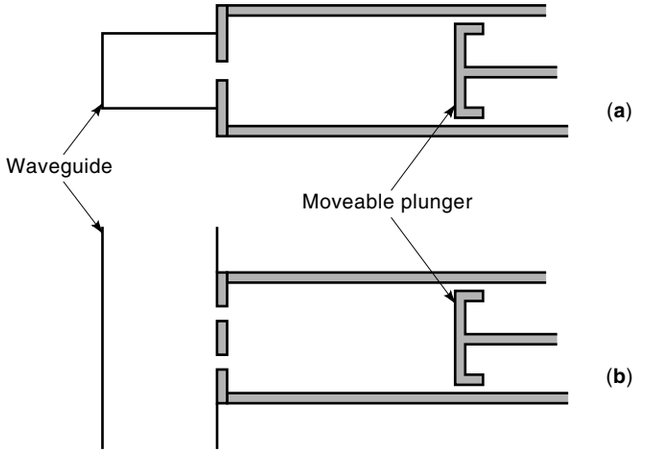

Figure 25. Cylindrical cavity wavemeter. (a) End view. (b) Top view.

whenever the cavity length is half a wavelength. Measuring the change in plunger positions between two successive minima and multiplying by two will give the wavelength of operation. Because of the large surface area of the coaxial outer wall, the cavity Q is not very high.

Cylindrical cavities are generally used for wavemeters, as shown in Fig. 25. The currents in the TM_{01} mode flow circumferential to the cavity cross section. Therefore, the shorting plunger does not need to have a good contact and provides easy manufacturability. Furthermore, other higher-order modes that require current flow in the end plates are not supported. In order to prevent other modes from being excited, two coupling holes in the side wall of a waveguide, which are a half wavelength apart, are used. The bandwidth of the coupling structures can be increased by selecting an elongated hole.

BIBLIOGRAPHY

1. R. E. Collin, *Foundations of Microwave Engineering,* New York: McGraw-Hill, 1966, chap. 7.
2. S. Ramo, J. Whinnery, and T. Van Duzer, *Fields and Waves in Communication Electronics,* New York: Wiley, 1965, chap. 10.
3. R. N. Ghose, *Microwave Circuit Theory and Analysis,* New York: McGraw-Hill, 1963, chap. 8.
4. T. Moreno, *Microwave Transmission Design Data,* New York: Dover, 1958, chap. 18.
5. H. J. Reich et al., *Microwave Principles,* Princeton, NJ: Van Nostrand, 1960, chap. 7.
6. J. G. Kretzschmar, Wave propagation in hollow conducting elliptic waveguide, *IEEE Trans. Microw. Theory Tech.,* **MTT-18**: 547–554, 1970.
7. J. G. Kretzschmar, Mode chart for elliptical resonant cavities, *Electron. Lett.,* **6**: 432–433, 1970.
8. W. Bräckelmann, Die Grenzfrequenzen von höheren Wellentypen im Koaxial Kabel mit elliptischem Querschnitt, *Arch. Elek. Übertragung.,* **21**: 421–426, 1967.
9. N. W. McLachlan, *Theory and Application of Mathieu Functions,* Oxford, England: Clarendon Press, 1947.
10. W. W. Hansen and R D. Richtmyer, On resonators suitable for klystron oscillators, *J. Appl. Phys.,* **10**: 189–199, 1939.

11. F. L. Ng, Tabulation of methods for the numerical solution of the hollow waveguide problem, *IEEE Trans. Microw. Theory Tech.,* **MTT-22**: 322–329, 1974.
12. E. L. Ginzton, *Microwave Measurements,* New York: McGraw-Hill, 1957, chap. 9.
13. I. Bahl and P. Bhartia, *Microwave Solid State Circuit Design,* New York: Wiley, 1988, chap. 3.
14. M. Sucher and J. Fox, *Handbook of Microwave Measurements,* 3rd ed., vol. 2, New York: Wiley, 1963, chap. 8.

Reading List

B. Lax and K. J. Button, *Microwave Ferrites and Ferromagnetics,* New York: McGraw-Hill, 1962, pp. 145–196.
S. Y. Liao, *Microwave Devices and Circuits,* Englewood Cliffs, NJ: Prentice-Hall, 1980, chap. 4.
P. F. Mariner, *Introduction to Microwave Practice,* New York: Academic Press, 1961, Chap. 7.
G. L. Matthaei, L. Young, and E. M. T. Jones, *Microwave Filters, Impedance Matching Networks and Coupling Structures,* New York: McGraw-Hill, 1964.
S. R. Rengarajan and J. E. Lewis, Quality factor of elliptical cylindrical resonant cavities, *J. Microw. Power,* **15**: 53–57, 1980.
A. K. Sharma, Spectral domain analysis of elliptic microstrip ring resonator, *IEEE Trans. Microw. Theory Tech.,* **MTT-32**: 212–218, 1984.
A. K. Sharma and B. Bhat, Spectral domain analysis of elliptic microstrip disk resonators, *IEE Trans. Microw. Theory Tech.,* **MTT-28**: 573–576, 1980.

ARVIND K. SHARMA
TRW

CAVITY RESONATORS, SUPERCONDUCTING. See SUPERCONDUCTING CAVITY RESONATORS.

CD-I. See OPTICAL CD-ROMS FOR CONSUMER ELECTRONICS.

CDMA. See CODE DIVISION MULTIPLE ACCESS.

CD-R. See OPTICAL CD-ROMS FOR CONSUMER ELECTRONICS.